Enhanced mast cell activation in mice deficient in the A2b adenosine receptor

Xiaoyang Hua,[1] Martina Kovarova,[1,2] Kelly D. Chason,[1] MyTrang Nguyen,[2] Beverly H. Koller,[1,2] and Stephen L. Tilley[1]

[1]Department of Medicine, Division of Pulmonary and Critical Care Medicine and [2]Department of Genetics, University of North Carolina at Chapel Hill, Chapel Hill, NC 27599

Antigen-mediated cross-linking of IgE bound to mast cells via the high affinity receptor for IgE triggers a signaling cascade that results in the release of intracellular calcium stores, followed by an influx of extracellular calcium. The collective increase in intracellular calcium is critical to the release of the granular contents of the mast cell, which include the mediators of acute anaphylaxis. We show that the sensitivity of the mast cell to antigen-mediated degranulation through this pathway can be dramatically influenced by the A2b adenosine receptor. Loss of this G_s-coupled receptor on mouse bone marrow–derived mast cells results in decreased basal levels of cyclic AMP and an excessive influx of extracellular calcium through store-operated calcium channels following antigen activation. Mice lacking the A2b receptor display increased sensitivity to IgE-mediated anaphylaxis. Collectively, these findings show that the A2b adenosine receptor functions as a critical regulator of signaling pathways within the mast cell, which act in concert to limit the magnitude of mast cell responsiveness when antigen is encountered.

CORRESPONDENCE
Stephen Tilley:
stephen_tilley@med.unc.edu

Abbreviations used: ADA, adenosine deaminase; ANOVA, analysis of variance; BMMC, bone marrow–derived mast cell; dbcAMP, dibutyryl cAMP; DNP, dinitrophenyl; DNP-HSA, DNP–human serum albumin; ES, embryonic stem; FcεRI, high affinity receptor for IgE; GPCR, G protein–coupled receptor; HMC-1, human leukemia mast cell line; NECA, adenosine-5′-*N*-ethylcarboxamide; NSCC, nonselective cation channels; PCA, passive cutaneous anaphylaxis; PKA, protein kinase A; PSA, passive systemic anaphylaxis; SOCC, store-operated calcium channel; TG, tharpsigargin; VSMC, vascular smooth muscle cell.

Mast cell activation is central to the pathophysiology of allergic asthma and other IgE-mediated diseases and has more recently been shown to regulate both innate and adaptive immune responses (1, 2). Cross-linking of IgE receptors by antigen triggers signaling through the high affinity receptor for IgE (FcεRI) on mast cells and results in mast cell degranulation, lipid mediator production, and cytokine synthesis. Several other biological mediators can influence the magnitude of mast cell activation through this classical stimulatory pathway.

Adenosine is a ubiquitous mediator that has long been recognized to influence mast cell function through activation of adenosine receptors on the cell surface (3). Mast cells express the A2a, A2b, and A3 adenosine receptors, and based on their differential G protein coupling, it has been widely assumed that stimulation of each receptor could influence mast cell function in different ways (4–7). Of all of the adenosine receptors discovered to date, the biological functions of A2b have been the most difficult to discern by pharmacological methods alone because of the difficulty in synthesizing agonists selective for this receptor subtype, as well as its capacity to couple to more than one G protein under conditions of forced expression and in some poorly differentiated mast cell lines (4, 8–11). As a result, investigators have relied on combinatorial pharmacological approaches with nonselective A2b agonists and more selective receptor antagonists to ascribe function to this adenosine receptor subtype (4, 10, 12–14).

Using this approach, a proinflammatory role for A2b on mast cells has been suggested by studies with the human leukemia mast cell line (HMC-1) and canine mastocytoma mast cell lines (BR cell lines) (4, 10, 13). In HMC-1 cells, although neither A2a nor A3 selective agonists increased proinflammatory cytokine release, the nonselective adenosine receptor agonist adenosine-5′-*N*-ethylcarboxamide (NECA) increased IL-8 release, and this effect was blocked by the A2b-selective antagonist enprofylline. In the BR cell line, NECA, but not an A3-selective agonist, could induce degranulation. This effect of NECA could be blocked by the A2b-selective antagonist enprofylline. Although these studies suggest that A2b receptors can mediate the proinflammatory effects of adenosine on HMC-1 cells, it remains unknown whether these findings are relevant and operative in the intact organism and how adenosine

The online version of this article contains supplemental material.

via A2b may influence antigen-induced mast cell activation, because these poorly differentiated cell lines do not express functional FcεRI receptors (15–17).

To determine the biological role of A2b on mast cells, we generated mice lacking the A2b adenosine receptor and have examined its contribution to antigen-induced mast cell activation in vitro and to antigen-induced anaphylaxis in vivo. Our data show that the A2b adenosine receptor functions as a negative regulator of mast cell activation by influencing cyclic nucleotide homeostasis and intracellular calcium influx into the mast cell.

RESULTS

Generation and characterization of A2b$^{-/-}$ mice

Mice carrying a mutant *A2b* allele were generated from 129/SvEv embryonic stem (ES) cells in which homologous recombination was used to replace part of the intron and the entirety of exon 2 (amino acids 113–332) with a marker gene (Fig. 1 A). Chimeric offspring carrying the mutant *A2b* locus were identified by Southern blot analysis of tail biopsies and bred with C57BL/6 females (Fig. 1 B). After six consecutive crosses to C57BL/6, mice heterozygous for the mutation were intercrossed to generate homozygous congenic N6 A2b$^{-/-}$ mice and A2b$^{+/+}$ littermate controls. Examination of mRNA prepared from the brain and kidney of the A2b$^{-/-}$ mice showed the absence of the normal *A2b* transcripts present in RNA preparations from A2b$^{+/+}$ animals (Fig. 1 C). We also analyzed the transcriptional production of the *A2b* gene in A2b$^{-/-}$ bone marrow–derived mast cells (BMMCs) by quantitative RT-PCR. As shown in Fig. 1 D, *A2b* expression was undetectable in cells from A2b$^{-/-}$ animals. In contrast, *A2b* was abundantly expressed in BMMCs from A2b$^{+/+}$ mice.

A2b$^{-/-}$ mice were born at expected Mendelian frequencies, appeared healthy, and were grossly indistinguishable from A2b$^{+/+}$ littermates. They achieve normal body weights and survive >1 yr. Both male and female A2b$^{-/-}$ mice have normal fertility. Histological analysis of all major organs revealed no anatomical developmental abnormalities as a result of A2b inactivation. Specific to this investigation, the number and morphology of mast cells in all tissues examined did not differ from that of A2b$^{+/+}$ littermate controls (Table I). Evaluation of conscious, unchallenged mice by tail cuff revealed that blood pressure and pulse were similar between A2b$^{-/-}$ mice and A2b$^{+/+}$ controls (systolic pressure: A2b$^{-/-}$ = 116.3 ± 2.5 mmHg and A2b$^{+/+}$ = 117.9 ± 3.7 mmHg [P = 0.72]; pulse: A2b$^{-/-}$ = 620.3 ± 10 bpm and A2b$^{+/+}$ = 639.8 ± 9.8 bpm [P = 0.2]), which suggests that, unlike the A2a receptor, the A2b receptor does not contribute to normal blood pressure homeostasis (18).

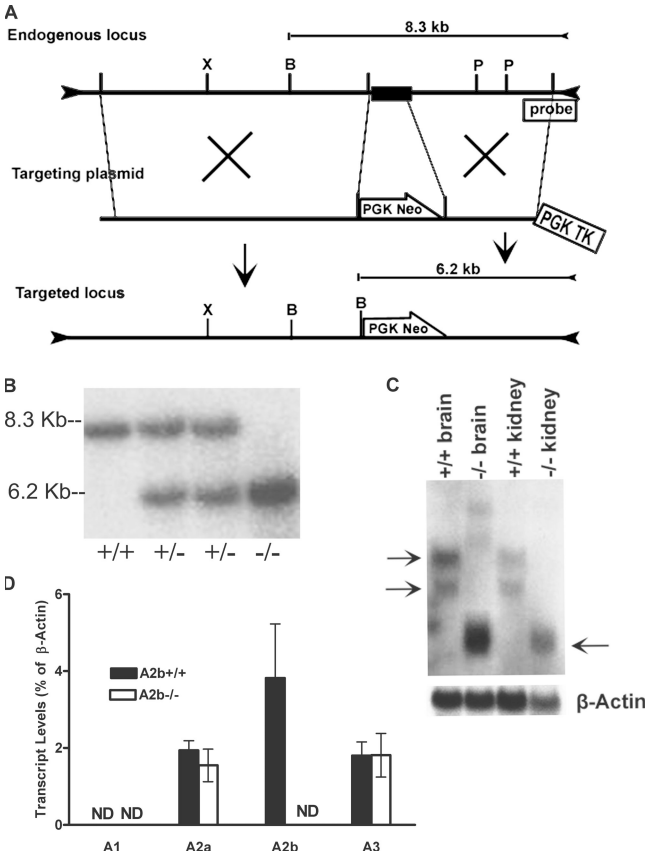

Figure 1. Targeted disruption of the mouse *A2b* gene. (A) The targeted disruption strategy consists of a targeting plasmid and genomic organization of the endogenous locus and targeted locus. The targeting plasmid is designed to disrupt the *A2b* gene by homologous recombination. The closed box represents exon 2 of the A2b gene, and the phosphoglycerate kinase–thymidine kinase (PGK-TK) and PGK-Neo selection cassettes are indicated by empty boxes. Restriction sites are abbreviated as follows: X, *Xba I*; B, *BamH I*; and P, *Psi I*. The location of the 3′ external probe used to detect homologous recombination events for the Southern blot analysis is indicated. (B) Southern blot analysis of *BamH I*–digested mouse genomic DNA from tail biopsies. Blots were hybridized with the radiolabeled 1-kb probe outside of the targeted region of the *A2b* gene, resulting in an 8.3-kb band for the endogenous locus and a band shift to 6.2 kb for the targeted locus. (C) Northern blot analysis of *A2b* mRNA in A2b$^{-/-}$ and A2b$^{+/+}$ mice. Total RNA extracts from the brain and kidney of A2b$^{-/-}$ and A2b$^{+/+}$ mice were isolated and hybridized with a [^{32}P]UTP-labeled cDNA probe (top) and β-actin probe (bottom) as loading controls. The arrows on the left indicate the two transcripts from the A2b$^{+/+}$ mice, and the arrow on the right shows the presence of the truncated transcript in the targeted locus. 20 μg of total RNA was loaded for each lane. (D) Quantitative RT-PCR analysis of mRNA level of adenosine receptors in A2b$^{+/+}$ versus A2b$^{-/-}$ BMMCs. Data are expressed as the mean transcript level ± SEM from three sets of A2b$^{-/-}$ and three sets of A2b$^{+/+}$ cells. ND, no transcripts detected.

Enhanced anaphylaxis in A2b$^{-/-}$ mice

To evaluate the role of the A2b receptor on mast cells, passive anaphylaxis was examined by two models. In these mast cell–dependent models, exogenously administered IgE is passively taken up by mast cells, and degranulation is evoked by the subsequent administration of antigen. Passive systemic anaphylaxis (PSA) was elicited by intravenous injection of 20 μg anti-dinitrophenyl (DNP) IgE. After 24 h, mice received DNP–human serum albumin (DNP-HSA) antigen by intravenous injection. Core body temperature was recorded as a

Table I. Mast cell histology in $A2b^{-/-}$ and $A2b^{+/+}$ mice

Organ	Numbers of mast cells (per mm^2)	
	$A2b^{+/+}$	$A2b^{-/-}$
Ear pinnae	43.9 ± 1.8	45.8 ± 2.6
Back skin	16 ± 0.8	18.5 ± 2.1
Tongue	10.6 ± 1.2	11.9 ± 2.4
Trachea	4.9 ± 1.1	5.3 ± 0.37
Stomach	6.7 ± 0.6	5.4 ± 0.48

monitor of the magnitude of the systemic anaphylactic response. As shown in Fig. 2 A, a greater temperature drop was observed in $A2b^{-/-}$ than in $A2b^{+/+}$ animals (4.6 ± 0.24 vs. 3.7 ± 0.29°C 10 min after DNP-HSA injection [$P = 0.03$]; 6.9 ± 0.36 vs. 5.6 ± 0.28°C 20 min after DNP-HSA injection [$P = 0.007$]). Surprisingly, ~30% of $A2b^{-/-}$ mice died after antigen challenge, whereas all $A2b^{+/+}$ animals survived, as expected, throughout the duration of the experiment ($P = 0.049$). As a result of this unexpected increase in the severity of the anaphylactic response with standard doses of IgE, all subsequent PSA experiments with $A2b^{-/-}$ mice were performed with lower amounts of IgE loading. As shown in Fig. 2 B, a more severe anaphylactic response was also observed in $A2b^{-/-}$ animals with a 10-fold lower dose (2 μg) of anti-DNP IgE ($P = 0.034$).

To further establish whether the A2b receptor might play an important in vivo role in the regulation of mast cell function, mice were evaluated in a second model of IgE/mast cell–dependent anaphylaxis, passive cutaneous anaphylaxis (PCA). PCA was elicited by subcutaneous injection of anti-DNP IgE into the pinna of the right ear. As an internal control, left ears were injected with the identical volume of vehicle. After 24 h, mice received antigen together with Evans blue dye by intravenous injection. Mast cell–induced plasma protein exudation can be quantitated in this model by determining the levels of dye in tissue biopsies from IgE-treated ears compared with those treated with vehicle. As shown in Fig. 3, Evans blue levels in biopsies from vehicle-treated pinnae was no different between $A2b^{-/-}$ and $A2b^{+/+}$ mice, suggesting that disruption of the A2b receptor did not modify basal vasopermeability. In contrast, extravasation in the IgE-treated pinnae was significantly higher than that present in vehicle-treated tissue in both $A2b^{-/-}$ and $A2b^{+/+}$ mice, reflecting degranulation of mast cells by cross-linking of the FcεRI-bound anti-DNP IgE by antigen. Significantly greater plasma extravasation was observed in pinnae from $A2b^{-/-}$ animals loaded with 1 ng IgE ($P = 7.36 \times 10^{-6}$), suggesting enhanced antigen-induced mast cell degranulation in these genetically modified animals. However, when the IgE dose was increased to 100 ng, plasma protein extravasation into the pinnae of $A2b^{+/+}$ mice approached that seen in $A2b^{-/-}$ animals ($P = 0.33$).

To establish that our in vivo findings were the result of A2b deficiency on mast cells, mast cell–deficient C57BL/6 $kit^{W\text{-}sh/W\text{-}sh}$ mice were reconstituted with $A2b^{+/+}$ or $A2b^{-/-}$

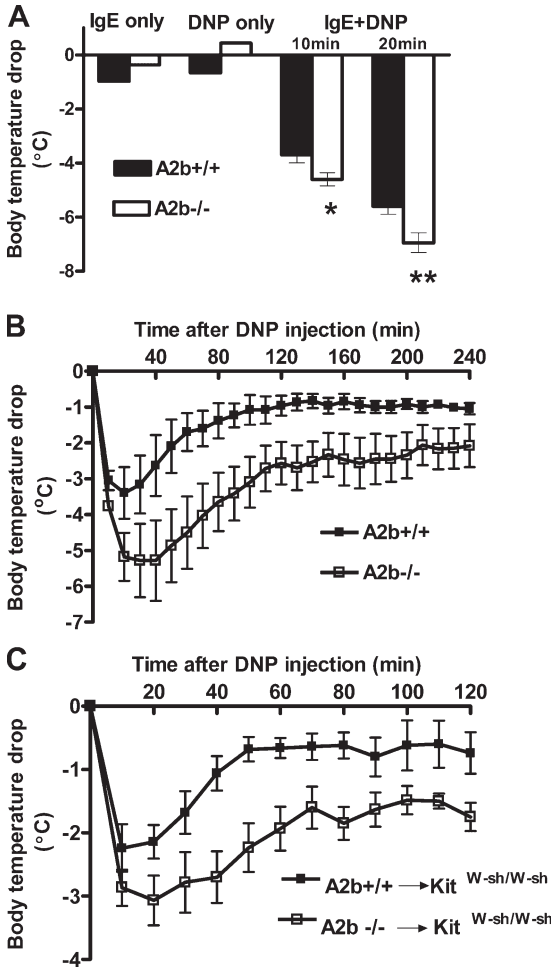

Figure 2. PSA in $A2b^{+/+}$, $A2b^{-/-}$, and reconstituted C57BL/6 $kit^{W\text{-}sh/W\text{-}sh}$ mice. Mice were intravenously loaded with 20 μg (A, $n = 14$ per group; and C, $n = 5$–6 per group) or 2 μg (B, $n = 6$ per group) of anti-DNP IgE and challenged with DNP-HSA 24 h later. Data represent the mean body temperature drop over time after DNP-HSA challenge ± SEM. $P < 0.05$ by repeated measurement analysis of variance (ANOVA; A– C). *, $P < 0.05$; and **, $P < 0.01$ versus $A2b^{+/+}$ mice by *t* test.

BMMCs (referred to as $A2b^{+/+} \rightarrow kit^{W\text{-}sh/W\text{-}sh}$ and $A2b^{-/-} \rightarrow kit^{W\text{-}sh/W\text{-}sh}$ mice, respectively). 8 mo after reconstitution, PSA experiments were performed as described. As shown in Fig. 2 C, $A2b^{-/-} \rightarrow kit^{W\text{-}sh/W\text{-}sh}$ mice showed more severe anaphylactic response than $A2b^{+/+} \rightarrow kit^{W\text{-}sh/W\text{-}sh}$ mice ($P < 0.05$), establishing that A2b deficiency on mast cells was indeed responsible for the enhanced anaphylactic response observed in $A2b^{-/-}$ mice. Collectively, these data derived from two mast cell–dependent models of anaphylaxis show that the A2b receptor functions as a negative regulator of mast cell degranulation in vivo by enhancing the sensitivity of the animal to the anaphylactic response elicited by antigen.

Enhanced antigen-induced degranulation of $A2b^{-/-}$ BMMCs

To determine the mechanism underlying our in vivo observations, in vitro experiments were performed with cultured

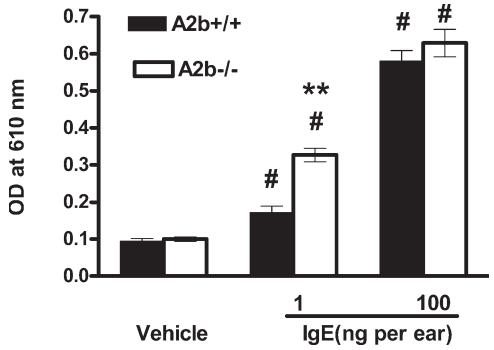

Figure 3. PCA in A2b$^{+/+}$ and A2b$^{-/-}$ mice. Mice were intradermally injected in the right ears with anti-DNP IgE in 20 μl PBS and in the left ears with aliquot vehicle. DNP-HSA/Evans blue solution was intravenously administered 24 h later, and Evans blue extravasation into the ears was measured. Data represent the mean OD ± SEM (n = 10 mice per group). #, $P < 0.0001$ versus vehicle-treated ears by t test; **, $P = 7.36 \times 10^{-6}$ versus A2b$^{+/+}$ ears by t test.

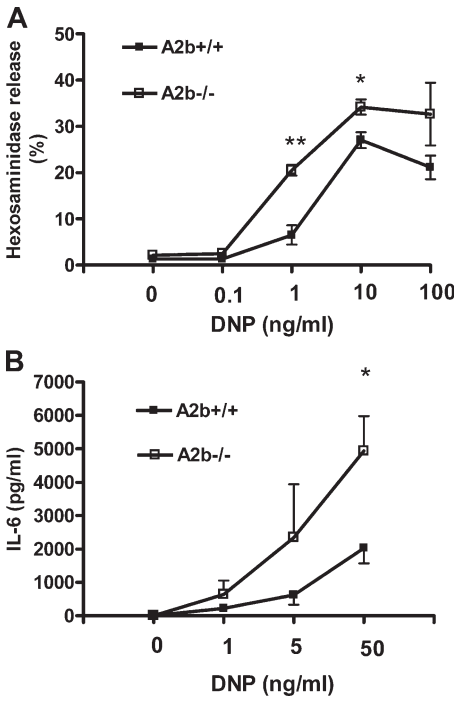

Figure 4. Antigen-induced degranulation and cytokine production from A2b$^{+/+}$ and A2b$^{-/-}$ mast cells. (A) Degranulation of BMMCs was assessed by measuring hexosamindase release from cells incubated with anti-DNP IgE after stimulation with increasing doses of DNP-HSA antigen. Data are from three different experiments using three different pairs of cells and are expressed as the mean percent hexosamindase release ± SEM. $P < 0.001$ by ANOVA. *, $P < 0.05$; and **, $P < 0.005$ versus A2b$^{+/+}$ cells by t test. (B) Cytokine production by BMMCs was evaluated by measuring IL-6 release 7 h after antigen stimulation. Cells were incubated with anti-DNP IgE and stimulated with 1, 5, or 50 ng/ml DNP-HSA antigen or vehicle, and cytokine levels were determined by ELISA. Data are from four different experiments using three different pairs of cells and are expressed as the mean IL-6 protein level ± SEM. $P < 0.05$ by ANOVA. *, $P < 0.05$ versus A2b$^{+/+}$ cells by t test.

BMMCs. BMMC cultures were established from 14 different A2b$^{-/-}$ mice animals and 14 A2b$^{+/+}$ littermate controls. The growth properties and granule content (determined by total hexosaminidase levels after cell lysis with Triton X-100) was examined in three of these lines. Morphologically, mast cells obtained from A2b$^{-/-}$ mice were indistinguishable from those obtained from A2b$^{+/+}$ animals, and flow cytometric analysis of the cultures after 5 wk with antibody directed against the FcεRI receptor showed similar numbers of positive cells, as well as similar levels of receptor expression (Fig. S1 A, available at http://www.jem.org/cgi/content/full/jem.20061372/DC1). To determine the impact of loss of the A2b receptor on antigen-induced mast cell degranulation, we measured hexosaminidase release from DNP-HSA antigen-stimulated BMMCs that had been cultured overnight in media containing anti-DNP IgE (Fig. 4 A). At low doses of antigen (1 ng/ml), only a modest increase in hexosaminidase release above basal levels was observed in BMMCs from A2b$^{+/+}$ mice (from 1.3 ± 0.12 to 6.5 ± 2.1%). In contrast, a sevenfold increase in hexosaminidase release above baseline was observed in BMMCs from A2b$^{-/-}$ animals (from 2.2 ± 0.6 to 20.5 ± 1.2%). Dose-response curves with DNP-HSA antigen showed enhanced release in A2b$^{-/-}$ BMMCs from 1–100 ng/ml ($P = 0.0009$).

Enhanced antigen-induced IL-6 release from A2b$^{-/-}$ BMMCs

In addition to releasing preformed mediators of anaphylaxis, mast cells also synthesize and secrete proinflammatory cytokines upon activation. To determine whether the A2b adenosine receptor could modify proinflammatory cytokine production from mast cells, IL-6 levels were measured in the supernatants of immunologically activated BMMCs. After incubation with antigen for 7 h, BMMCs lacking the A2b receptor released higher amounts of IL-6 than those from A2b$^{+/+}$ animals at several different concentrations of antigen ($P < 0.05$; Fig. 4 B).

A3 signaling in A2b$^{-/-}$ mast cells

Because we have previously shown that activation of A3 receptors by exogenous adenosine can potentiate antigen-induced degranulation of mast cells, we surmised that enhanced signaling of endogenous adenosine through the A3 receptor, either through up-regulated expression or function, could explain the increased sensitivity of the A2b$^{-/-}$ mice to antigen (6, 19). As shown in Fig. 1 D, A3 expression was not up-regulated in the absence of A2b receptors. Because a previous report has suggested that the A2b receptor may serve as an alternate anchoring protein of ecto–adenosine deaminase (ADA), the primary metabolic enzyme of adenosine, we postulated that enhanced antigen-induced degranulation of BMMCs from A2b$^{-/-}$ mice could be because of less activity of ecto-ADA on A2b$^{-/-}$ cells (20). In the absence of ecto-ADA, it is possible that endogenous adenosine levels could be elevated and potentiate antigen-induced degranualation through the A3 receptor. To address this possibility, we

treated A2b$^{-/-}$ cells with the potent A3 selective antagonist VUF5574 to determine whether antigen-induced degranulation would be attenuated. 50 nM to 100 μM VUF5574 failed to inhibit antigen-induced degranulation of BMMCs from A2b$^{-/-}$ mice (Fig. S2, available at http://www.jem.org/cgi/content/full/jem.20061372/DC1), suggesting that the enhanced antigen-induced degranulation of BMMCs observed in A2b$^{-/-}$ mice was not the result of increased signaling through A3 receptors.

FcεRI expression on A2b$^{-/-}$ mast cells

To determine whether or not enhanced A2b$^{-/-}$ mast cell sensitivity to antigen could be caused by up-regulated expression of FcεRI, we evaluated FcεRI expression on both cultured BMMCs and freshly collected peritoneal mast cells. Because IgE sensitization can increase FcεRI expression, we measured both basal and IgE–up-regulated FcεRI expression on these cells. For basal level evaluation, cultured BMMCs or freshly collected peritoneal mast cells from both A2b$^{-/-}$ and A2b$^{+/+}$ mice were incubated with fluorescently tagged IgE antibody for 30 min, and flow cytometry was performed. As shown in Fig. S1 (A and B), no differences in basal FcεRI expression were detected between A2b$^{-/-}$ and A2b$^{+/+}$ mast cells. For IgE–up-regulated FcεRI expression, both A2b$^{-/-}$ and A2b$^{+/+}$ mice were sensitized by IgE through the tail vein, and peritoneal mast cells were collected and analyzed by flow cytometry 24 h later. As shown in Fig. S1 B, FcεRI expression was up-regulated to a similar degree in A2b$^{-/-}$ and A2b$^{+/+}$ mast cells. These data indicate that enhanced antigen sensitivity in A2b$^{-/-}$ mice is not caused by up-regulated FcεRI expression.

Intracellular cAMP in BMMCs

To determine the mechanism by which disruption of the A2b receptor up-regulates mast cell function, we investigated the cAMP levels in BMMCs from A2b$^{-/-}$ mice and A2b$^{+/+}$ controls. Activation of A2b receptors has been shown to increase intracellular cAMP levels in diverse cell lines; we thus posited that, in the absence of A2b receptors, cAMP levels could be reduced (21). As shown in Fig. 5, cAMP levels were significantly lower in A2b$^{-/-}$ BMMCs at the baseline and after antigen stimulation.

Enhanced intracellular calcium influx in A2b$^{-/-}$ BMMCs

Because calcium influx is an essential trigger for exocytosis, we measured intracellular cytoplasmic calcium concentration ($[Ca^{2+}]_i$) in A2b$^{+/+}$ and A2b$^{-/-}$ BMMCs loaded with Fura-2 AM, a specific indicator of free calcium. In A2b$^{+/+}$ cells, $[Ca^{2+}]_i$ increased after antigen stimulation with 20 ng/ml DNP-HSA to five times the basal level (from 50 to 250 nM), whereas in A2b$^{-/-}$ BMMCs, $[Ca^{2+}]_i$ increased to nine times the basal level (from 50 to 450 nM; Fig. 6 A). To determine if the enhanced $[Ca^{2+}]_i$ response observed after antigen stimulation in A2b$^{-/-}$ cells was caused by up-regulation of ER calcium stores or calcium entry from outside of the cells, we activated BMMCs with antigen in calcium-free buffer.

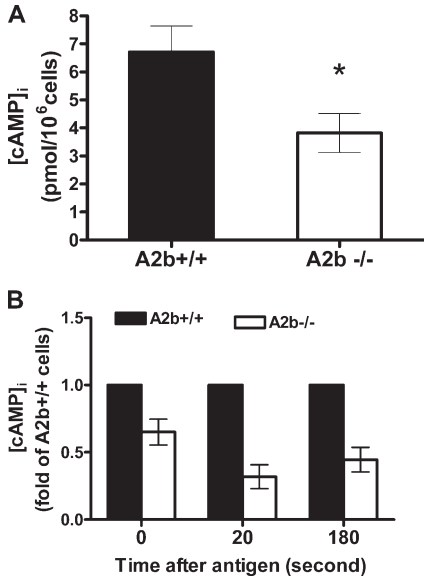

Figure 5. Intracellular cAMP levels in A2b$^{+/+}$ and A2b$^{-/-}$ mast cells. (A) Basal cAMP level in BMMCs from A2b$^{+/+}$ and A2b$^{-/-}$ mice was determined by ELISA. Data are from three separate experiments using three sets of cells and are expressed as the mean ± SEM. *, P = 0.03 versus A2b$^{+/+}$ cells by *t* test. (B) cAMP level in both A2b$^{-/-}$ and A2b$^{+/+}$ mast cells at the indicated times after DNP challenge. Data are expressed as fold cAMP level relative to A2b$^{+/+}$ cells, ± SEM.

As shown in Fig. 6 B, antigen initiated a small $[Ca^{2+}]_i$ increase (two times the basal level), which was not different between A2b$^{+/+}$ and A2b$^{-/-}$ cells. However, after the addition of extracellular calcium (final concentration = 1 mM), calcium influx was 1.5 times higher in A2b$^{-/-}$ cells compared with A2b$^{+/+}$ cells. To further verify a role for extracellular calcium influx in the enhanced sensitivity of A2b$^{-/-}$ mast cells, we stimulated cells with tharpsigargin (TG), a specific inhibitor of the ER calcium-ATPase. TG treatment in calcium-free buffer results in passive release of ER calcium stores, independent of upstream signaling events. The TG treatment increased $[Ca^{2+}]_i$ to a similar extent in A2b$^{-/-}$ and A2b$^{+/+}$ cells suspended in calcium-free buffer. The reintroduction of calcium resulted in a greater influx (1.9 times) of calcium in A2b$^{-/-}$ cells compared with A2b$^{+/+}$ cells (Fig. 6 C). These results suggest an enhanced function of store- operated calcium channels (SOCCs) in A2b$^{-/-}$ cells. Next, we examined the effects of surrogate Ca^{2+} ions: Sr^{2+} and Ba^{2+}. Ca^{2+} surrogates are able to pass through all known store-operated channels (22) but are not substrates for Ca^{2+} transporters and do not activate most Ca^{2+}-dependent processes to the same extent as Ca^{2+}. As shown in Fig. 6 D, depletion of calcium stores with TG followed by addition of Sr^{2+} ions at a final concentration of 1 mM resulted in an increase in 340:380 nm fluorescence ratio. Interestingly, this ratio was only 1.3 times higher in A2b$^{-/-}$ compared with A2b$^{+/+}$ cells. Similar results were found when Ba^{2+} was used (not depicted). The lower difference in 340:380 nm ratio between A2b$^{-/-}$ and

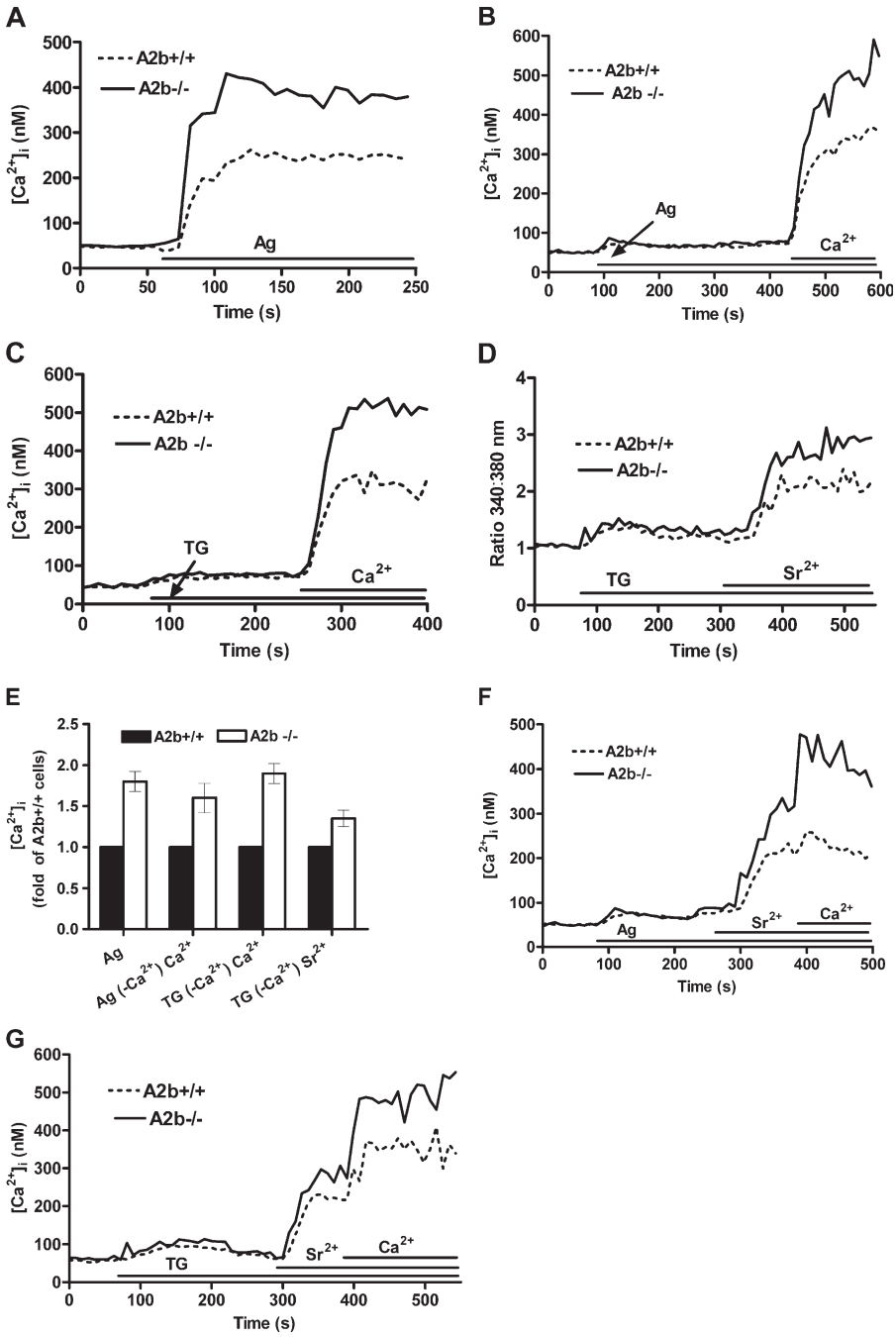

Figure 6. Calcium influx in A2b$^{+/+}$ and A2b$^{-/-}$ mast cells. (A–C) Calcium influx in A2b$^{+/+}$ and A2b$^{-/-}$ BMMCs (anti-DNP IgE preloaded) in calcium (A) or calcium-free (B and C) buffer were treated with 20 ng/ml DNP-HSA (A and B) or 1 μM TG (C) and, cytosolic-free calcium was measured as shown. When cells were suspended in calcium-free buffer, extracellular calcium was repleted to final a concentration of 1 mM after DNP-HSA or TG challenge. (D) Increased Ca^{2+} surrogate Sr^{2+} influx in A2b$^{-/-}$ cells. A2b$^{+/+}$ or A2b$^{-/-}$ BMMCs in calcium-free buffer were challenged with 1 μM TG, and Sr^{2+} was added to a final concentration of 1 mM. Sr^{2+} influx was recorded as shown. (E) Mean fold increase of intracellular Ca^{2+} or Sr^{2+} concentrations, ± SEM, in A2b$^{-/-}$ cells compared with A2b$^{+/+}$ cells after FcεRI-mediated activation. (F and G) Increased Ca^{2+} surrogate Sr^{2+} influx in A2b$^{-/-}$ cells. A2b$^{-/-}$ and A2b$^{+/+}$ BMMCs (anti-DNP IgE preloaded) in calcium-free buffer were triggered by DNP-HSA (F) or TG (G), and bivalent cations were recovered by successive addition of 1 mM Sr^{2+} and 1 mM Ca^{2+} as shown. Representative results from at least three independent experiments and two sets of cells are shown. Ag, antigen.

$A2b^{+/+}$ cells in the presence of Sr^{2+} or Ba^{2+} compared with Ca^{2+} suggested that the A2b receptor may influence both nonselective cation channels (NSCCs) and SOCCs. This was further supported by the observations that mixtures of Ca^{2+}/Sr^{2+} ions further increased the 340:380 nm fluorescence ratio compared with Sr^{2+} or Ba^{2+} alone. Differences in response between $A2b^{-/-}$ and $A2b^{+/+}$ mast cells increased from 1.3 in the presence of Sr^{2+} only to 1.7 in the presence of Ca^{2+}/Sr^{2+} mixtures (Fig. 6 F). Similar results were found with TG (Fig. 6 G). Interestingly, extracellular calcium influx in $A2b^{-/-}$ and $A2b^{+/+}$ mast cells was blocked when 10 μM La^{3+} was added in the presence of Ca^{2+}, Sr^{2+}, or Ca^{2+}/Sr^{2+} ions (not depicted). Collectively, these findings show that the A2b receptor regulates store-operated calcium influx into the mast cell and suggest that these effects are not isolated to a specific calcium channel.

Effects of dibutyryl cAMP (dbcAMP) on degranulation and antigen-induced calcium influx in $A2b^{-/-}$ and $A2b^{+/+}$ mast cells

To investigate whether the observed alteration in cAMP could be mechanistically related to the changes in mast cell

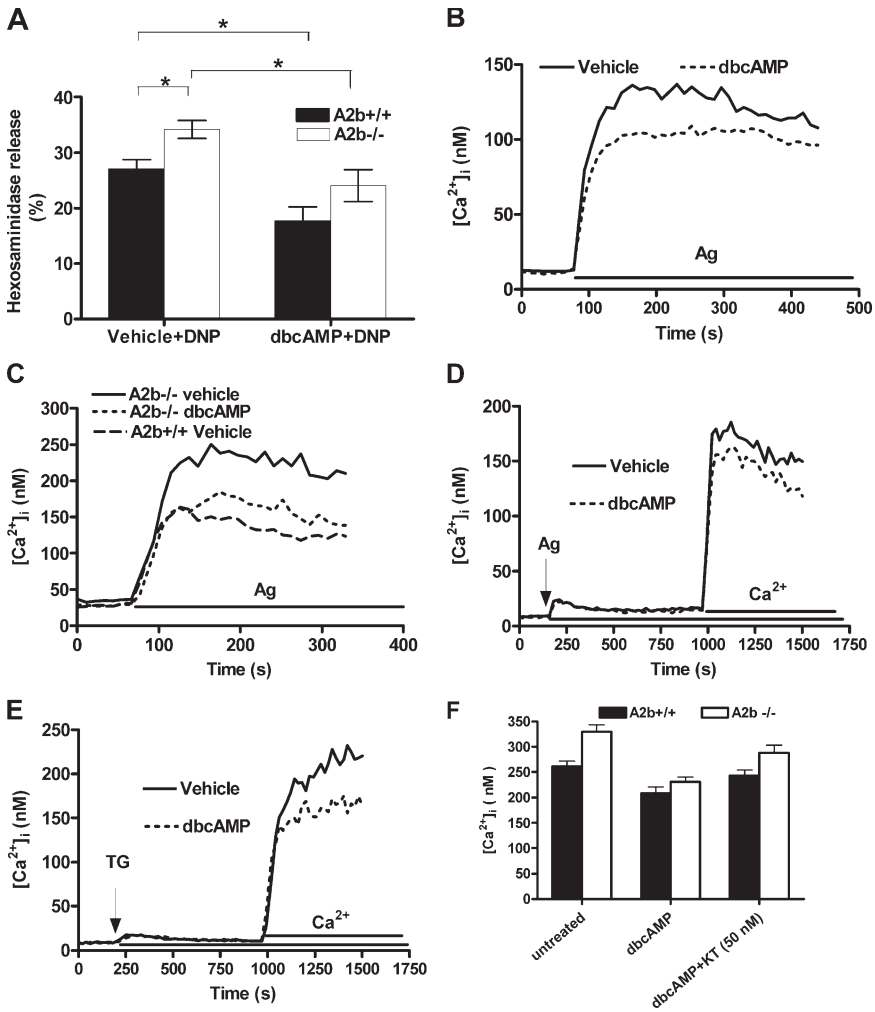

Figure 7. Inhibitory effect of cAMP analogue on hexosaminidase release and SOCCs on mast cells. (A) Inhibitory effect of cAMP analogue on antigen-induced degranulation of both $A2b^{+/+}$ and $A2b^{-/-}$ mast cells. Anti-DNP IgE preloaded $A2b^{-/-}$ and $A2b^{+/+}$ BMMCs were treated with 3 mM dbcAMP for 30min before the challenge with 10 ng/ml DNP, and the effect of dbcAMP on antigen-induced degranulation of $A2b^{-/-}$ and $A2b^{+/+}$ BMMCs was measures as shown. Data represent mean hexosaminidase release, ± SEM, from four separated experiments using three different sets of cells. *, $P < 0.05$ by *t* test. (B–E) Inhibitory effect of cAMP analogue on antigen- (B–D) or TG-induced (E) calcium influx in both $A2b^{+/+}$ and $A2b^{-/-}$ mast cells. Both $A2b^{-/-}$ and $A2b^{+/+}$ BMMCs in calcium (B and C) or calcium-free (D and E) buffer were treated with dbcAMP buffer were treated with dbcAMP and DNP-HSA (B–D), or TG-induced (E) calcium influx was recorded. When cells were suspended in calcium-free buffer (D and E), extracellular calcium was restored 10 min after the addition of antigen (D) or TG (E). Representative results from at least three independent experiments and two sets of cells are shown. (F) Anti-DNP IgE preloaded $A2b^{-/-}$ and $A2b^{+/+}$ BMMCs were treated with 50 nM of PKA inhibitor KT5720 for 30 min, and the dbcAMP effect on antigen-induced calcium influx was reevaluated as shown. Data represent mean $[Ca^{2+}]_i$, ± SEM, from three independent experiments and two sets of cells. Ag, antigen.

degranulaion, hexosaminidase release in BMMCs was measured after treatment with dbcAMP. As shown in Fig. 7 A, dbcAMP treatment inhibited degranulation in $A2b^{+/+}$ and $A2b^{-/-}$ BMMCs. The mechanism behind these inhibitory effects of cAMP on mast cell degranulation are poorly understood (23–25). In our experiments, we observed that higher $[cAMP]_i$ in $A2b^{+/+}$ BMMCs relative to $A2b^{-/-}$ cells was associated with decreased extracellular calcium influx into the cell. To determine whether these alterations in cAMP and calcium might be related, we treated cells with the dbcAMP and observed its effects on calcium signaling. As shown in Fig. 7 B, treatment of $A2b^{+/+}$ BMMCs with the cAMP analogue reduced total calcium influx into the cell. Pretreatment of $A2b^{-/-}$ BMMCs with dbcAMP lowered the magnitude of calcium influx to that observed in $A2b^{+/+}$ cells (i.e., reduced the difference of antigen-driven calcium influx between $A2b^{-/-}$ and $A2b^{+/+}$ cells; Fig. 7 C). When cells were suspended in calcium-free buffer, the release of internal calcium stores was minimally or not affected by dbcAMP treatment, but influx of extracellular calcium was reduced after store depletion by antigen or TG (Fig. 7, D and E). Collectively, these results suggest that cAMP levels within the mast cell can influence antigen-induced mast cell degranulation by altering calcium influx through SOCCs on the cell membrane. To further elucidate the mechanism by which cAMP modifies SOCCs, we pretreated BMMCs with the protein kinase A (PKA) inhibitor KT5720 before addition of dbcAMP. As shown in Fig. 7 F, 50 nM KT5720 inhibited dbcAMP-mediated attenuations of calcium influx, suggesting that the effect of cAMP on SOCC channel activity is indirect via a PKA-dependent mechanism.

DISCUSSION

Mast cell activation mediated by FcεRI is a critical event in the allergic inflammatory response. The potency of adenosine as a modulator of mast cell function is well recognized, and adenosine receptors are of considerable interest as therapeutic targets for asthma and allergy (9, 26). Although in vitro studies have suggested roles for each adenosine receptor on the mast cell, the biological function of these receptors on mast cells in vivo, particularly A2b receptors, is largely unknown (5, 19, 21). In this study we show, using mice lacking the A2b receptor, a surprising nonredundant role for this adenosine receptor as a negative regulator of mast cell function. Mice lacking the A2b receptor demonstrated heightened susceptibility to antigen-induced anaphylaxis. In vitro studies with cultured mast cells from these same animals showed greater calcium influx through SOCCs after activation with antigen, which correlated with enhanced degranulation and cytokine production. cAMP levels were markedly lower in mast cells from $A2b^{-/-}$ mice, suggesting that A2b-G_s signaling may be of fundamental importance in the constitutive control of cyclic nucleotide levels within mast cells, and by extension a critical regulator of cellular activation.

Our results are in contrast to findings with HMC-1 cells in which the A2b receptor has been shown to subserve a proinflammatory role. Feoktistov et al. reported that the nonselective adenosine analogue NECA could induce IL-8 released from HMC-1 cells. Lack of such an effect by the A2a-selective agonist CGS21680, failure of an A3 receptor antagonist to abolish the response, and blockade of NECA-induced IL-8 release by either 300 μM enprofylline or 3-isobutyl-8-pyrrolidinoxanthine suggested that A2b receptors were mediating this action of adenosine in this cell line (4, 12, 13). A2b receptor activation on HMC-1 cells results in mobilization of intracellular calcium through a G_q-coupled signaling pathway, potentially explaining the capacity of this receptor to transmit a proinflammatory signal in this cell line (4). Similar findings of A2b-linked calcium mobilization have been found in canine mastocytoma cells, with NECA-induced degranulation attributed to activation of the A2b receptor (10). To our knowledge, A2b-mediated calcium mobilization in mast cells has only been observed under conditions of forced expression in transfection experiments and in some poorly differentiated mast cell lines, which have many acquired phenotypic differences from normal, nonmalignant mast cells, most notably their lack of FcεRI and their different profiles of ion channels (15–17, 27, 28). Our previous data have shown that either A3 receptor deletion or A3 selective antagonism could totally abolish adenosine-induced calcium influx in both BMMCs (unpublished data) and primary lung mast cells, suggesting that A2b-G_q coupling may be a unique feature of these manipulated and malignant mast cell lines (7).

Although our study is the first to use a genetic approach to characterize the function of A2b on mast cells, many studies support an antiinflammatory role for this receptor on other immune cells. First, the A2b receptor has been shown to couple to G_s proteins in all cells types examined (21). Elevations in cAMP, as the result of adenylate cyclase activation, have been repeatedly shown to inhibit the function of immune cells, including mast cells (23–25, 29). Second, in human T lymphocytes, A2b receptors are up-regulated after lymphocyte activation by phytohemagglutinin or anti–T cell receptor–CD3 complex antibodies and are functional as IL-2 production is reduced by NECA but not by the A2a-selective agonist CGS21680 (30). Finally, both pharmacological and genetic studies have attributed adenosine-mediated inhibition of macrophage function to A2b. In A2a receptor–deficient mice, A2b receptors have been shown to inhibit TNF release induced by thioglycollate, and up-regulated A2b expression correlates with increases in cAMP production in mouse macrophages treated with adenosine receptor agonists; IFN-γ–induced proinflammatory cytokine release by macrophages is inhibited by activation of A2b receptor; and adenosine can increase antiinflammatory cytokine IL-10 release by macrophage (14, 31, 32). Recently, genetic studies have also shown an inhibitory role for A2b receptors on macrophages. Yang et al. found up-regulated release of multiple proinflammatory cytokines by mouse macrophages lacking the A2b receptor under both basal conditions and after activation by LPS (33). Collectively, our findings and those

described in this section support an antiinflammatory function of A2b receptors on immune cells.

A surprising finding from our studies was the marked reduction in basal cAMP levels in BMMCs isolated from $A2b^{-/-}$ animals. There are at least two possible explanations for this finding. First, autocrine and paracrine adenosine produced in the BMMC cultures could activate A2b receptors on the mast cell surface and contribute to the maintenance of cyclic nucleotide levels within the cell. In the absence of A2b, this signal would be lost and cAMP levels might fall. However, because of the low affinity of this receptor for adenosine, it is unlikely that endogenous adenosine at physiological levels would be capable of activating the A2b receptor. A second and more plausible explanation for our findings is that the A2b receptor may have intrinsic, spontaneous activity. The capacity of G protein–coupled receptors (GPCRs) to achieve a constitutively active conformation in the absence of ligand is well recognized; however, the level of such activity differs among GPCRs (34, 35). For example, even the same GPCR can have different levels of constitutive activity independent of its intrinsic molecular properties, depending on the cell types on which it is expressed (35). Our data showing enhanced mast cell function in $A2b^{-/-}$ mice, but normal basal hemodynamics, suggest a constitutive role for A2b on mast cells but not vascular smooth muscle cells (VSMCs). Indeed, it has recently been shown that VSMCs lacking A2b receptors have similar basal levels of cAMP compared with $A2b^{+/+}$ VSMCs (33). The concept of constitutive activation of A2b receptors on mast cells raises important questions about the use of A2b antagonists in asthmatics. A2b antagonists with inverse agonist activity could result in the lowering of cAMP levels within the mast cell, potentially enhancing antigen-induced degranulation and proinflammatory cytokine production.

Antigen-induced mast cell degranulation is a well-coordinated event requiring several essential steps, including the cross-linking of IgE by antigen, activation of tyrosine kinases by FcεRI, and, finally, fusion of mast cell granules with the cell membrane (36, 37). Critical to this fusion event is the influx of extracellular calcium through SOCCs, activated when calcium stores are depleted by the interaction of inositol trisphosphate with the endoplasmic reticulum (2, 38). In our studies, enhanced degranulation of $A2b^{-/-}$ BMMCs was associated with enhanced extracellular calcium influx. To investigate whether reduced cAMP levels could be linked to enhanced calcium influx, we examined calcium signaling after pharmacological manipulation of cAMP within BMMCs. In our studies we found an inhibitory effect of the cAMP analogue dbcAMP on the antigen-induced cytosolic-free calcium increase in BMMCs, which was achieved by reducing the calcium influx from the extracellular matrix rather than by inhibiting calcium release from the ER. This inhibitory effect of dbcAMP on extracellular calcium influx was verified when we observed similar results in BMMCs treated with the ER calcium-depleting agent TG. These findings not only imply that the enhanced antigen-driven calcium influx in $A2b^{-/-}$ BMMCs may be attributable to the lower cAMP level, they also provide a reasonable explanation for the widely accepted observation that increased cAMP levels are associated with impaired antigen-driven mast cell activity.

An inhibitory effect of cAMP on store-operated calcium influx has recently been shown in other cell lines. Ay et al. found that both cAMP analogues and forskolin, through the downstream kinase system, were able to inhibit calcium influx through $La3^{+}/Ni2^{+}$-sensitive SOCCs, which corresponded well with cAMP-induced airway dilation (39). The profile of calcium channels on mast cells, which is reported to include the NSCCs and SOCCs but varies among mast cell lines, has not yet been identified (27, 40). Both NSCCs and SOCCs on mast cells belong to the transient receptor potential family of channels, which is gated by the signal of ER calcium depletion and dependent on transmembrane potential difference (41). The mechanism by which cAMP influences SOCCs is unknown. One possibility is that cAMP influences SOCC activity indirectly by changing membrane potential through other ion channels. For example, in rat peritoneal mast cells, cAMP can elicit a delayed chloride ion influx, which results in hypopolarization of the mast cell membrane (41). However, recent experiments have shown that mast cells can also secrete chloride ion through the cAMP-gated cystic fibrosis transmembrane conductance regulator (42). The cAMP-driven chloride ion trans-membrane transit, which subsequently alters the transmembrane potential, is believed to considerably influence the magnitude of calcium influx into the cell. Potassium and sodium channels have also been identified on different mast cell lines and are believed to contribute to polarization of the cell membrane (27, 40). The exact roles of these ion channels on mast cells, and whether second messengers can modify their properties, are still areas of active investigation.

It has long been recognized that elevations of intracellular cAMP can inhibit mast cell function. However, the mechanism by which cyclic nucleotides regulate the function of mast cells is not well understood. Our data suggest that cAMP levels within the mast cell influence the activity of cell membrane–associated calcium channels, the final common pathways for cellular activation. Moreover, our studies have identified a nonredundant role for the G_s-coupled A2b adenosine receptor as a critical regulator of cAMP levels within mouse mast cells, with functional consequences of enhanced mast cell activation in its absence. If similar control of human mast cells is also attributable to the constitutive expression of A2b receptors, then these findings may have important implications as adenosine receptor ligands are developed and tested for the treatment of asthma and allergy.

MATERIALS AND METHODS

Animal welfare. The use of experimental animals was in accordance with the Institutional Animal Care and Use Committee guidelines of the University of North Carolina at Chapel Hill.

Generation of A2b-deficient mice. A 15-kb genomic region of the *A2b* gene was isolated from a mouse 129-phage library prepared from E14TG2a

ES cells and subsequently subcloned into pBluescript II KS(+). The plasmid pJNS2 was used to construct the *A2b* targeting vector by replacing a portion of the endogenous gene with a neomycin-resistant gene, resulting in the disruption of the *A2b* gene after homologous recombination. The targeted plasmid was linearized at the Not I site and introduced into the E14TG2a ES cell line by electroporation, and clones that were resistant to both G418 and gancyclovir were identified by standard methods, as previously described (43). Isolated clones were screened for the desired recombination event by Southern blot analysis. The positively targeted cell lines were microinjected into 3.5-d-old C57BL/6 blastocysts to generate chimeras that were capable of transmitting the mutant allele to their offspring. Male chimeras were mated to C57BL/6 females to generate heterozygous animals for the mutant allele. These heterozygous mice were subsequently backcrossed to C57BL/6 for six generations. After six generations of backcrosses, heterozygous mice were intercrossed to generate homozygous mice for the *A2b* mutation ($A2b^{-/-}$) and $A2b^{+/+}$ littermate controls ($A2b^{+/+}$).

Genotyping. Genomic DNA was isolated from ES cell clones and from tail biopsies of neonates by high salt precipitation and analyzed by genomic Southern blotting as previously described (19).

Northern blot analysis. Northern blot analysis of *A2b* mRNA in the brains and kidneys from $A2b^{-/-}$ and $A2b^{+/+}$ mice was performed as previously described (19).

Real-time RT-PCR analysis. Real-time RT-PCR for evaluation of expression of adenosine receptor subtypes on BMMCs from $A2b^{-/-}$ and $A2b^{+/+}$ mice was performed using a sequence detector (model 7700; Applied Biosystems) as previously described (7).

Blood pressure measurements. Systolic blood pressure and heart rate measurements were made in conscious mice using a noninvasive computerized tail-cuff system as previously described (44). For each mouse, eight measurements were performed in eight different channels on the tail-cuff system on a daily basis during eight consecutive days, and the mean of the eight measurements was taken as the data point of the mouse. Measurements were performed during a fixed time period each day.

PSA. PSA was performed as previously described (6). Mice were injected intravenously with 20 or 2 μg mouse anti-DNP IgE mAb (Sigma-Aldrich) via the tail vein. 24 h after IgE loading, 1 mg DNP-HSA was injected intravenously. Core body temperatures were recorded over time. Negative controls received either IgE + Evans blue or DNP-HSA + Evans blue. Investigators were blinded to genotype during all experiments.

PCA. PCA was performed as previously described (6). Animals were lightly anesthetized, and the right ears were injected intradermally with 1 or 100 ng anti-DNP IgE mAb in 20 μl PBS. The left ears were injected with 20 μl PBS. 24 h later, animals were injected intravenously with 100 μl of 1% Evan's blue dye containing 100 μg DNP-HSA. Animals were killed 90 min after intravenous injection, and ear biopsies were incubated in 1 ml formamide at 54°C for 48 h. Quantitative analysis of formamide extracts was determined by measuring the absorbance of Evans blue at 610 nm with a spectrophotometer. Investigators were blinded to genotype during all experiments.

BMMC culture, hexosaminidase release, and IL-6 measurement. BMMCs were isolated from 8–16-wk-old mice and grown in RPMI 1640 medium supplemented with 10% FCS, 20 ng/ml mouse IL-3, and 20 ng/ml stem cell factor, as previously described (45). Cell purity was determined by toluidine blue staining and flow cytometric analysis for FcεRI expression. Mast cell degranulation was determined by β-hexosaminidase activity assay as previously described (19). Antagonist, or cAMP analogue, if used before antigen introduction, was added as indicated in the figures. IL-6 measurement was performed by ELISA (Assay Design). Samples were prepared as previously described (46).

Mast cell histology. Mast cell histology was performed as previously described (6, 47). In brief, organs from three sets of $A2b^{-/-}$ and $A2b^{+/+}$ littermates were harvested and fixed in 10% formalin. After paraffin embedding, 5-μm sections were cut and stained with toluidine blue. Mast cells were recognized by positively staining cells and counted in a blinded fashion.

Reconstitution of mast cells. Reconstitution of $A2b^{-/-}$ and $A2b^{+/+}$ mast cells was performed as previously described (47). In brief, BMMCs from $A2b^{-/-}$ and $A2b^{+/+}$ littermate controls were cultured for 5 wk. Mice deficient in mast cells ($kit^{W\text{-}sh/W\text{-}sh}$) were reconstituted with six million of either $A2b^{-/-}$ or $A2b^{+/+}$ BMMCs by tail-vein injection. Reconstituted mice were housed in pathogen-free circumstance with 12 h of day/night shifts for 8 mo. Confirmation of mast cell reconstitution in these recipients was histologically confirmed by toluidine blue staining of tissues from several different organs.

Flow cytometric analysis. Flow cytometric analysis of FcεRI expression on BMMCs and freshly collected peritoneal mast cells from both $A2b^{-/-}$ and $A2b^{+/+}$ mice was performed as described previously (48).

Intracellular cAMP assay in BMMCs. Intracellular cAMP was measured as previously described with some modification (46). In brief, cells were washed with Tyrode's solution (137 mM NaCl, 2.7 mM KCl, 1 mM $MgCl_2$, 1.8 mM $CaCl_2$, 0.2 mM NaH_2PO_4, 12 mM $NaHCO_3$, and 5.5 mM D-Glucose) twice. Two million cells were lysed, and cAMP was measured using the Direct cAMP kit according to the manufacture's protocol (Assay Designs). For measurement of cAMP levels after DNP challenge, BMMCs were loaded with IgE mAb at 100 ng/ml/1×10^6 cells overnight. Cells were washed twice with Tyrode's buffer and resuspended at 2×10^7 cells/ml. One million cells were used and treated with DNP at 3 ng/ml for 20 s or 3 min. cAMP levels were determined as described in this section.

Intracellular calcium measurement. $[Ca^{2+}]_i$ was determined by a microplate reader (FLUOstar OPTIMA; BMG Labtechnologies), as previously described (45). In brief, BMMCs were loaded with mouse anti-DNP IgE overnight (100 ng/1×10^6 cells/ml). Cells were washed with calcium buffer (137 mM NaCl, 2.7 mM KCl, 0.2 mM NaH_2PO_4, 5.5 mM glucose, 1 mM $CaCl_2$, 1 mM $MgCl_2$, 12 mM $NaHCO_3$, 10 mM Hepes, and 0.1% BSA) twice and loaded with Fura-2 AM (1 μg/2×10^6 cells/ml) at 37°C for 40 min. After loading, cells were washed twice with calcium buffer, and 2×10^5 cells were transferred to black-wall 96-well microplates (Becton Dickinson). After basal $[Ca^{2+}]_i$ was determined, cells were challenged with DNP-HSA. In some experiments, cells were washed in calcium-free buffer (containing 0.2 mM EDTA), and cells were activated with DNP-HSA or TG after 2 min at 37°C. The extracellular Ca^{2+} was restored to 1 mM after an additional 5 min. For evaluation of Ca^{2+}-specific store-operated channel responses, 1 mM Sr^{2+} or 1 mM Ba^{2+} ions were used instead of Ca^{2+}. Real-time fluorescence signal was measured with excitement wavelengths 340 and 380 nm and with a constant emission at 510 nm. Intracellular calcium level was calculated as previously described (49). For Sr^{2+} and Ba^{2+} ions, the ratio of fluorescence in 340 and 380 nm was used instead of concentration. For data reported as fold increase between genotypes, calculations were done using the highest point in the curve.

cAMP analogue effect on SOCCs. cAMP analogue effect on SOCCs was also performed on the FLUOstar OPTIMA microplate reader. In brief, after IgE and Fura-2 AM loading, 2×10^5 cells in either calcium or calcium-free buffer were transferred to black-wall 96-well microplates and treated with 3 mM dbcAMP in distilled/deionized water. Controls were set up by adding aliquot vehicle only. 3 min later, cells was challenged with either antigen or TG and cytosolic-free calcium was monitored. Extracellular calcium was restored 10 min after the addition of stimulant when cells were in calcium-free buffer.

For preinhibition of PKA before dbcAMP addition, 50 nM of PKA inhibitor (KT5720; EMD Bioscience) was introduced into both $A2b^{-/-}$ and $A2b^{+/+}$ mast cells suspended in calcium buffer 30 min before dbcAMP treatment.

Online supplemental material. Fig. S1 A shows the expression of FcεRI receptors on cultured BMMCs from $A2b^{-/-}$ and $A2b^{+/+}$ mice. Fig. S1 B shows the expression of FcεRI receptors on freshly collected peritoneal mast cells from $A2b^{-/-}$ and $A2b^{+/+}$ mice. Fig. S2 shows the effect of A3-selective antagonist VUF5574 on antigen-induced activation of $A2b^{-/-}$ mast cells. Supplemental materials and methods describes mouse peritoneal lavage. Online supplemental material is available at http:www.jem.org/cgi/content/full/jem.20061372/DC1.

The authors would like to thank Dr. H.-S. Kim for the phage library, Dr. J. Snouwaert for work on the targeting construct, A. Latour for work with ES cells, Y. Brooks for mouse genotyping, and the Keck family for their generous support of the Keck Animal Models Facility at the University of North Carolina.

This work was supported by National Institutes of Health grants HL071802 (to S.L. Tilley) and HL080697 (to B.H. Koller).

The authors have no conflicting financial interests.

Submitted: 27 June 2006
Accepted: 4 December 2006

REFERENCES

1. Galli, S.J., S. Nakae, and M. Tsai. 2005. Mast cells in the development of adaptive immune responses. *Nat. Immunol.* 6:135–142.
2. Metcalfe, D.D., D. Baram, and Y.A. Mekori. 1997. Mast cells. *Physiol. Rev.* 77:1033–1079.
3. Marquardt, D.L., C.W. Parker, and T.J. Sullivan. 1978. Potentiation of mast cell mediator release by adenosine. *J. Immunol.* 120:871–878.
4. Feoktistov, I., and I. Biaggioni. 1995. Adenosine A2b receptors evoke interleukin-8 secretion in human mast cells. An enprofylline-sensitive mechanism with implications for asthma. *J. Clin. Invest.* 96:1979–1986.
5. Suzuki, H., M. Takei, T. Nakahata, and H. Fukamachi. 1998. Inhibitory effect of adenosine on degranulation of human cultured mast cells upon cross-linking of Fc epsilon RI. *Biochem. Biophys. Res. Commun.* 242:697–702.
6. Tilley, S.L., V.A. Wagoner, C.A. Salvatore, M.A. Jacobson, and B.H. Koller. 2000. Adenosine and inosine increase cutaneous vasopermeability by activating A(3) receptors on mast cells. *J. Clin. Invest.* 105:361–367.
7. Zhong, H., S.G. Shlykov, J.G. Molina, B.M. Sanborn, M.A. Jacobson, S.L. Tilley, and M.R. Blackburn. 2003. Activation of murine lung mast cells by the adenosine A3 receptor. *J. Immunol.* 171:338–345.
8. Linden, J., T. Thai, H. Figler, X. Jin, and A.S. Robeva. 1999. Characterization of human A(2B) adenosine receptors: radioligand binding, Western blotting, and coupling to G(q) in human embryonic kidney 293 cells and HMC-1 mast cells. *Mol. Pharmacol.* 56:705–713.
9. Jacobson, K.A., and Z.G. Gao. 2006. Adenosine receptors as therapeutic targets. *Nat. Rev. Drug Discov.* 5:247–264.
10. Auchampach, J.A., X. Jin, T.C. Wan, G.H. Caughey, and J. Linden. 1997. Canine mast cell adenosine receptors: cloning and expression of the A3 receptor and evidence that degranulation is mediated by the A2B receptor. *Mol. Pharmacol.* 52:846–860.
11. Yakel, J.L., R.A. Warren, S.M. Reppert, and R.A. North. 1993. Functional expression of adenosine A2b receptor in *Xenopus* oocytes. *Mol. Pharmacol.* 43:277–280.
12. Feoktistov, I., E.M. Garland, A.E. Goldstein, D. Zeng, L. Belardinelli, J.N. Wells, and I. Biaggioni. 2001. Inhibition of human mast cell activation with the novel selective adenosine A(2B) receptor antagonist 3-isobutyl-8-pyrrolidinoxanthine (IPDX)(2). *Biochem. Pharmacol.* 62:1163–1173.
13. Feoktistov, I., S. Ryzhov, A.E. Goldstein, and I. Biaggioni. 2003. Mast cell-mediated stimulation of angiogenesis: cooperative interaction between A2B and A3 adenosine receptors. *Circ. Res.* 92:485–492.
14. Xaus, J., M. Mirabet, J. Lloberas, C. Soler, C. Lluis, R. Franco, and A. Celada. 1999. IFN-gamma up-regulates the A2B adenosine receptor expression in macrophages: a mechanism of macrophage deactivation. *J. Immunol.* 162:3607–3614.
15. Nilsson, G., T. Blom, M. Kusche-Gullberg, L. Kjellen, J.H. Butterfield, C. Sundstrom, K. Nilsson, and L. Hellman. 1994. Phenotypic characterization of the human mast-cell line HMC-1. *Scand. J. Immunol.* 39:489–498.
16. Butterfield, J.H., D. Weiler, G. Dewald, and G.J. Gleich. 1988. Establishment of an immature mast cell line from a patient with mast cell leukemia. *Leuk. Res.* 12:345–355.
17. Garcia, G., P. Brazis, N. Majo, L. Ferrer, F. de Mora, and A. Puigdemont. 1998. Comparative morphofunctional study of dispersed mature canine cutaneous mast cells and BR cells, a poorly differentiated mast cell line from a dog subcutaneous mastocytoma. *Vet. Immunol. Immunopathol.* 62:323–337.
18. Ledent, C., J.M. Vaugeois, S.N. Schiffmann, T. Pedrazzini, M. El Yacoubi, J.J. Vanderhaeghen, J. Costentin, J.K. Heath, G. Vassart, and M. Parmentier. 1997. Aggressiveness, hypoalgesia and high blood pressure in mice lacking the adenosine A2a receptor. *Nature.* 388:674–678.
19. Salvatore, C.A., S.L. Tilley, A.M. Latour, D.S. Fletcher, B.H. Koller, and M.A. Jacobson. 2000. Disruption of the A(3) adenosine receptor gene in mice and its effect on stimulated inflammatory cells. *J. Biol. Chem.* 275:4429–4434.
20. Herrera, C., V. Casado, F. Ciruela, P. Schofield, J. Mallol, C. Lluis, and R. Franco. 2001. Adenosine A2B receptors behave as an alternative anchoring protein for cell surface adenosine deaminase in lymphocytes and cultured cells. *Mol. Pharmacol.* 59:127–134.
21. Feoktistov, I., and I. Biaggioni. 1997. Adenosine A2B receptors. *Pharmacol. Rev.* 49:381–402.
22. Ma, H.T., R.L. Patterson, D.B. van Rossum, L. Birnbaumer, K. Mikoshiba, and D.L. Gill. 2000. Requirement of the inositol trisphosphate receptor for activation of store-operated Ca2+ channels. *Science.* 287:1647–1651.
23. Torphy, T.J. 1998. Phosphodiesterase isozymes: molecular targets for novel antiasthma agents. *Am. J. Respir. Crit. Care Med.* 157:351–370.
24. Peachell, P.T., L.M. Lichtenstein, and R.P. Schleimer. 1991. Differential regulation of human basophil and lung mast cell function by adenosine. *J. Pharmacol. Exp. Ther.* 256:717–726.
25. Weston, M.C., and P.T. Peachell. 1998. Regulation of human mast cell and basophil function by cAMP. *Gen. Pharmacol.* 31:715–719.
26. Holgate, S.T. 2005. The Quintiles Prize Lecture 2004. The identification of the adenosine A2B receptor as a novel therapeutic target in asthma. *Br. J. Pharmacol.* 145:1009–1015.
27. Bradding, P., and E.C. Conley. 2002. Human mast cell ion channels. *Clin. Exp. Allergy.* 32:979–983.
28. Brazis, P., R. Torres, M. Queralt, F. de Mora, L. Ferrer, and A. Puigdemont. 2002. Evaluation of cell-surface IgE receptors on the canine mastocytoma cell line C2 maintained in continuous culture. *Am. J. Vet. Res.* 63:763–766.
29. Shichijo, M., N. Inagaki, M. Kimata, I. Serizawa, H. Saito, and H. Nagai. 1999. Role of cyclic 3′,5′-adenosine monophosphate in the regulation of chemical mediator release and cytokine production from cultured human mast cells. *J. Allergy Clin. Immunol.* 103:S421–S428.
30. Mirabet, M., C. Herrera, O.J. Cordero, J. Mallol, C. Lluis, and R. Franco. 1999. Expression of A2B adenosine receptors in human lymphocytes: their role in T cell activation. *J. Cell Sci.* 112:491–502.
31. Kreckler, L.M., T.C. Wan, Z.D. Ge, and J.A. Auchampach. 2006. Adenosine inhibits tumor necrosis factor-alpha release from mouse peritoneal macrophages via A2A and A2B but not the A3 adenosine receptor. *J. Pharmacol. Exp. Ther.* 317:172–180.
32. Nemeth, Z.H., C.S. Lutz, B. Csoka, E.A. Deitch, S.J. Leibovich, W.C. Gause, M. Tone, P. Pacher, E.S. Vizi, and G. Hasko. 2005. Adenosine augments IL-10 production by macrophages through an A2B receptor-mediated posttranscriptional mechanism. *J. Immunol.* 175:8260–8270.
33. Yang, D., Y. Zhang, H.G. Nguyen, M. Koupenova, A.K. Chauhan, M. Makitalo, M.R. Jones, C.S. Hilaire, D.C. Seldin, P. Toselli, et al. 2006. The A(2B) adenosine receptor protects against inflammation and excessive vascular adhesion. *J. Clin. Invest.* 116:1913–1923.
34. Milligan, G. 2003. Constitutive activity and inverse agonists of G protein-coupled receptors: a current perspective. *Mol. Pharmacol.* 64:1271–1276.

35. Seifert, R., and K. Wenzel-Seifert. 2002. Constitutive activity of G-protein-coupled receptors: cause of disease and common property of wild-type receptors. *Naunyn Schmiedebergs Arch. Pharmacol.* 366:381–416.
36. Tkaczyk, C., and A.M. Gilfillan. 2001. Fc(epsilon)Ri-dependent signaling pathways in human mast cells. *Clin. Immunol.* 99:198–210.
37. Seino, S., and T. Shibasaki. 2005. PKA-dependent and PKA-independent pathways for cAMP-regulated exocytosis. *Physiol. Rev.* 85:1303–1342.
38. Parekh, A.B., and J.W. Putney Jr. 2005. Store-operated calcium channels. *Physiol. Rev.* 85:757–810.
39. Ay, B., A. Iyanoye, G.C. Sieck, Y.S. Prakash, and C.M. Pabelick. 2006. Cyclic nucleotide regulation of store-operated Ca2+ influx in airway smooth muscle. *Am. J. Physiol. Lung Cell. Mol. Physiol.* 290:L278–L283.
40. Bradding, P. 2005. Mast cell ion channels. *Chem. Immunol. Allergy.* 87:163–178.
41. Penner, R., G. Matthews, and E. Neher. 1988. Regulation of calcium influx by second messengers in rat mast cells. *Nature.* 334:499–504.
42. Kulka, M., M. Gilchrist, M. Duszyk, and A.D. Befus. 2002. Expression and functional characterization of CFTR in mast cells. *J. Leukoc. Biol.* 71:54–64.
43. Mohn, A., and B.H. Koller. 1995. Genetic manipulation of embryonic stem cells. *In* DNA Cloning: A Practical Approach. Second edition. D.M. Glover and B.D. Hames, editors. Oxford University Press, New York. 143–184.
44. Krege, J.H., J.B. Hodgin, J.R. Hagaman, and O. Smithies. 1995. A noninvasive computerized tail-cuff system for measuring blood pressure in mice. *Hypertension.* 25:1111–1115.
45. Kovarova, M., C.A. Wassif, S. Odom, K. Liao, F.D. Porter, and J. Rivera. 2006. Cholesterol deficiency in a mouse model of Smith-Lemli-Opitz syndrome reveals increased mast cell responsiveness. *J. Exp. Med.* 203:1161–1171.
46. Nguyen, M., M. Solle, L.P. Audoly, S.L. Tilley, J.L. Stock, J.D. McNeish, T.M. Coffman, D. Dombrowicz, and B.H. Koller. 2002. Receptors and signaling mechanisms required for prostaglandin E2-mediated regulation of mast cell degranulation and IL-6 production. *J. Immunol.* 169:4586–4593.
47. Grimbaldeston, M.A., C.C. Chen, A.M. Piliponsky, M. Tsai, S.Y. Tam, and S.J. Galli. 2005. Mast cell-deficient W-sash c-kit mutant kit W-sh/W-sh mice as a model for investigating mast cell biology in vivo. *Am. J. Pathol.* 167:835–848.
48. Ryan, J.J., S. DeSimone, G. Klisch, C. Shelburne, L.J. McReynolds, K. Han, R. Kovacs, P. Mirmonsef, and T.F. Huff. 1998. IL-4 inhibits mouse mast cell Fc epsilonRI expression through a STAT6-dependent mechanism. *J. Immunol.* 161:6915–6923.
49. Petr, M.J., and R.D. Wurster. 1997. Determination of in situ dissociation constant for Fura-2 and quantitation of background fluorescence in astrocyte cell line U373-MG. *Cell Calcium.* 21:233–240.